Micromechanical contribution for the prediction of the viscoelastic properties of high rate recycled asphalt and influence of the level blending

A. Eddhahak [a,*], M. Vandamme [b], V.T. Vu [b]

[a] Laboratory PIMM, CNRS UMR 8006, Arts et métiers ParisTech, 151 boulevard de l'hôpital, 75013 Paris, France
[b] Université Paris-Est, Laboratoire Navier (UMR 8205), CNRS, ENPC, IFSTTAR, 77455 Marne-la-Vallée, France

ABSTRACT

This research deals with an experimental and micromechanical study of high rate recycled asphalt with 70% of RAP. Rheological measurements of shear complex modulus of virgin, RAP and blended binders were performed at different temperatures and frequencies. Then, a micromechanical model based on the generalized self-consistent scheme (GSCS) was suggested for the prediction of the effective mechanical properties of the recycled asphalt. The GSCS-based approach aims to homogenize the heterogeneous material taking into account the intergranular porosity, on the one hand, and the possible interactions between its phases on the other one. The suggested method was compared to a step-by-step (successive) homogenization approach and literature data in elastic case were used for this purpose. The results have shown that the GSCS-based approach presents a good agreement with the data especially for higher volume fractions of aggregates. Furthermore, the significant influence of the blend homogeneity level on the estimation of the effective mechanical properties of the recycled asphalt was highlighted.

1. Introduction

Pavement recycling has been increasingly gaining a great attention in the asphalt industry. In addition to the ecological benefits and the natural resources preservation, recycling allows also the reduction of energy consumption resulting therefore in a more cost-effective production and considerable economical gains [1,2]. In France, since the oil crisis of 1973, the bituminous materials have been more and more recovered for recycling and competitive efforts are made to involve high amounts of RAP (reclaimed asphalt pavement). Nowadays, RAP rates up to 30% are commonly used in the road construction and rehabilitation projects making thereby necessary to control the properties of the final recycled product [3].

In this context, some research works have focused on the investigation of the viscoelastic properties of the recycled asphalt from different point of views. Eddhahak-Ouni et al. [4,5] have presented an experimental laboratory protocol based on a progressive extraction combined with a FTIR spectroscopy analysis in order to highlight the relationship

between the manufacture recycling process on the one hand and the level of homogeneity of the blended binder on the other one. They concluded that the temperature and the time mixing parameters involved in the asphalt manufacture shall be well calibrated in order to reach the wished blending level of the final binder and to control thereby the mechanical performances of the recycled asphalt. Other research works suggested empirical and analytical predictive models for the prediction of the viscoelastic properties of the asphaltic concrete based upon the rheological information of its bituminous binder and mix design [6–9]. Some of these models have shown some limitations for specific solicitation frequency and temperature ranges [10] and others often require complementary experimental tests on the asphaltic concrete [11].

Although they are reliable, the experimental-based approaches are sometimes very long and cumbersome to perform. Furthermore, experiences can be costly and too much time and energy-consuming especially when dealing with the investigation of the material responses under different mechanical scenarios. For these reasons, innovative approaches based on the rational mechanics have been adopted in opposition of the so-called empiric school. The micromechanics which has been developed for decades is a complementary approach whose purpose is to provide efficient deductive tools for the prediction of the effective properties of the heterogeneous material based on the knowledge of the properties of its constituents. It was highlighted with the help of the extensive literature that micromechanics can be used to understand the mechanical behavior of the bituminous materials. Buttlar et al. [12] used the generalized self-consistent scheme (GSCS) model [13,14] in order to investigate the asphalt mastic behavior. Later, Shashidar and Shenoy [15] suggested a modified form of Buttlar solution involving the use of an order of magnitude analysis for simplification of the complex sets of the GSCS equations. The research of Lachihab [16] considered the asphalt as a biphase composite including spherical inclusions coated by a bitumen film and embedded in the infinite equivalent medium. Nevertheless, the intergranular porosity was not taken into account in his work. More recently, Alam and Hammoum [17] presented a micromechanical analysis based on a successive homogenization process in which the self-consistent model was considered in three multiscale steps for the prediction of the viscoelastic properties of HMA mixes. However, errors up to 50% were recorded in some cases for the prediction of the mechanical behavior of the asphalt. From the above studies, the suitability of the generalized self-consistent model was shown and its reliability to provide good predictions of the equivalent properties of the composite [18], but further work is still needed for a better prediction of the asphalt properties.

In this framework, the objectives of the present work are:

(i) To present a novel micromechanical approach based on the GSCS model and illustrated on a laboratory case of a high rate recycled HMA including 70% of RAP. The intergranular porosity of the composite is taken into account in the modeling.
(ii) To investigate the level of blending of the final binder and its influence in the prediction of the viscoelastic properties of the high rate recycled HMA.

2. Theoretical development

The recycled asphalt is a heterogeneous material composed of typically 95% (by mass) of aggregates and 5% of bituminous binder. Thus, this composite can be assumed as a multiphase material reinforced by elastic inclusions (aggregates ''a'') which are surrounded by a viscoelastic matrix (mastic ''m'') and weakened by the porosity phase (air voids ''p'') (Fig. 1). Accordingly, the micromechanical model which will be considered here is based on the generalized self-consistent scheme (GSCS) [16]. This model was initially formulated by Christensen and Lo [13] for two-phase materials through a 3-phase scheme by considering a composite spherical inclusion coated by a matrix shell which is embedded in an equivalent homogeneous infinite medium (EHM). Unlike the classic self-consistent scheme, the GSCS is an implicit model since the final solution is expressed as a function of the properties of the EHM which is unknown in itself. For further information on this micromechanical scheme, the reader could consult the detailed work of Hervé and Zaoui [14].

In addition, for a better and more accurate definition of the multiphase composite, conclusions have been drawn from the previous research of Navaro [19] through which it was highlighted that in the case of a good blending of the virgin binder into the RAP-binder, the aggregate is surrounded by just one homogeneous binder layer (Fig. 2a). Accordingly, in the case of a ''good'' blending configuration, one can suppose a monolayer spherical inclusion of a (2 + 1)-phase micromechanical model [20]. Whereas, in the case of a ''bad'' blending of virgin and RAP binders, a 2-layered inclusion is considered. The first layer close to the aggregate corresponds to the RAP binder and the second layer is relative to the virgin binder (Fig. 2b). Accordingly, a (3 + 1)-phase model will be adopted for the description of this configuration. In the following, the micromechanical development based on the $(n + 1)$-phase model ($n = 2, 3$) is presented in order to appreciate the effective homogeneous mechanical properties of the recycled asphalt composite in both configurations (good and bad blending levels). For the sake of simplicity, the problem will be first tractable in the case of linear elasticity and the solution is then extended to the viscoelasticity.

2.1. The GSCS-based approach (elasticity case)

In this section, we will assume that the heterogeneous material is composed with purely elastic phases; thereby the associated representative volume element (RVE), denoted as ''Ω'', is described by a first elastic spherical inclusion (corresponding to the aggregates) coated by an elastic phase and a second spherical inclusion (corresponding to the
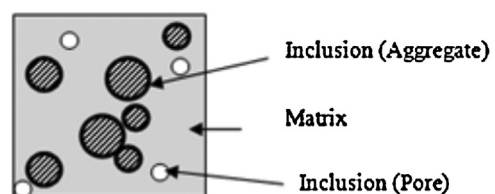

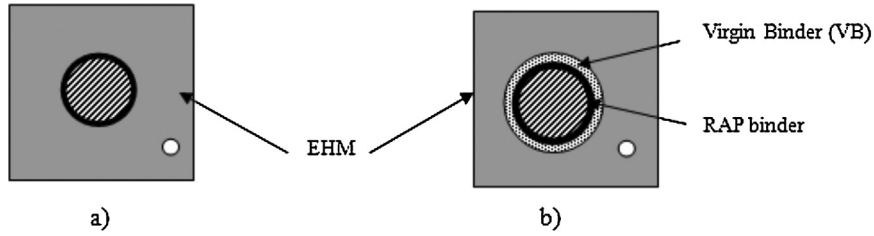Fig. 1 – Schematic modeling of the asphaltic concrete.

Fig. 2 – GSCS representations of recycled asphaltic concretes. (a) Monolayer case (good blending) and (b) bi-layer case (bad blending).
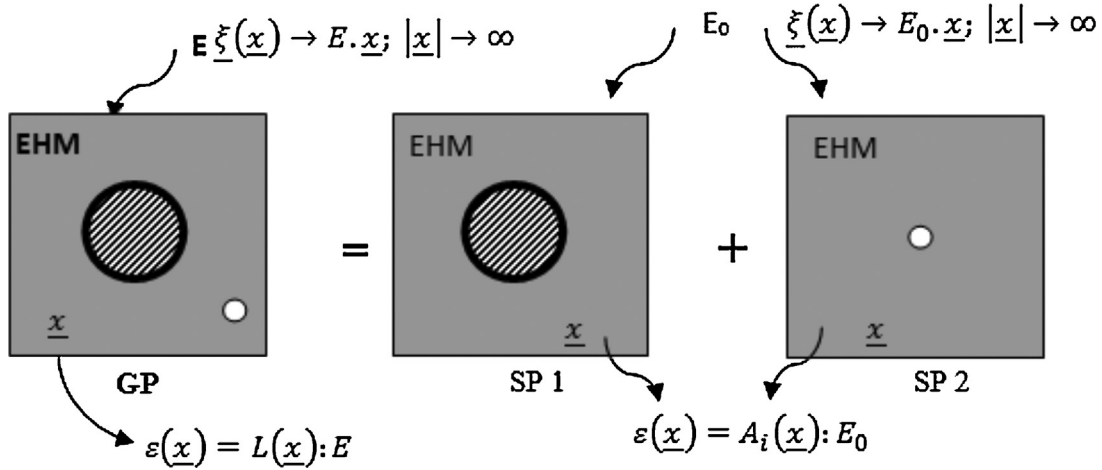

Fig. 3 – Illustration of the tractability of the homogenization global problem "GP".

porosity) which are embedded in an equivalent homogeneous infinite phase subjected to uniform strain condition **E** at infinity. Each phase is characterized by a bulk modulus k_i, a Poisson's ratio υ_i, a shear modulus μ_i and a volume fraction f_i. Note that k_i and μ_i are equal to zero for the particular case of the porosity.

The homogenization global problem denoted "GP" can then be solved by considering simultaneously two secondary problems named "SP1" and "SP2", associated respectively to the rigid inclusion (aggregates) and the "weak" inclusion (porosity) and subjected to the same auxiliary deformation $\mathbf{E_0}$ at infinity (Fig. 3).

As known, the prediction of the homogeneous equivalent mechanical properties of a heterogeneous material by a multiscale approach requires the knowledge of the average of the localization tensors of each phase of the composite according to the following:

$$\textbf{complexes;}^{hom} = \langle \textbf{complexes;} : A \rangle = \sum_i f_i \textbf{complexes;}_i : \langle \mathbb{A}_i \rangle \tag{1}$$

where **complexes;**^{hom} and **complexes;**$_i$ are respectively the effective and the local stiffness 4th-order tensors; $\mathbb{A}_i$ is the strain localization 4th-order tensors of the phase i associated to the secondary problem. In the case of the global problem, the average strain localization tensor, denoted $\mathbb{L}$, is defined as the parameter that relates the micro-strain field ε of each point of micro-coordinate x of the RVE to the macro-strain field **E** applied at infinity:

$$\varepsilon_i(\mathbf{x}) = \langle \mathbb{L}_i(\mathbf{x}) \rangle : \mathbf{E} \tag{2}$$

As a matter of the fact, the localization problem has to be solved at first for the derivation of the homogenized properties. Based on the fact that the average strain ε equals the macro-strain **E** on the one hand and the average sum of the strains relative to the different phases on the other hand, it can be easily demonstrated that the strain localization tensor of the global problem is related to that of the secondary problems according to the following:

$$\langle \mathbb{L}_i(\mathbf{x}) \rangle = \langle \mathbb{A}_i \rangle : \left(\sum_i f_i \langle \mathbb{A}_i \rangle \right)^{-1} \tag{3}$$

By assuming that the material is isotropic and making use of the spherical symmetry of the problem, the micro-strain field of the secondary configurations can be obtained by the resolution of two elementary problems of simple shear and hydrostatic pressure applied at infinity. Note that in the case of linear isotropy, the stiffness tensor is given by:

$$\textbf{complexes;} = 3\kappa \mathbb{I}^{\textbf{vol}} + 2\mu \mathbb{I}^{\textbf{dev}} \tag{4}$$

where κ and μ are respectively the elastic bulk and shear moduli whereas $\mathbb{I}^{vol}$ and $\mathbb{I}^{dev}$ denote respectively the spherical and deviatoric operators.

By considering a displacement approach with boundary displacements conditions, one can determine the average strain in each phase for both uniform and deviatoric strain conditions as:
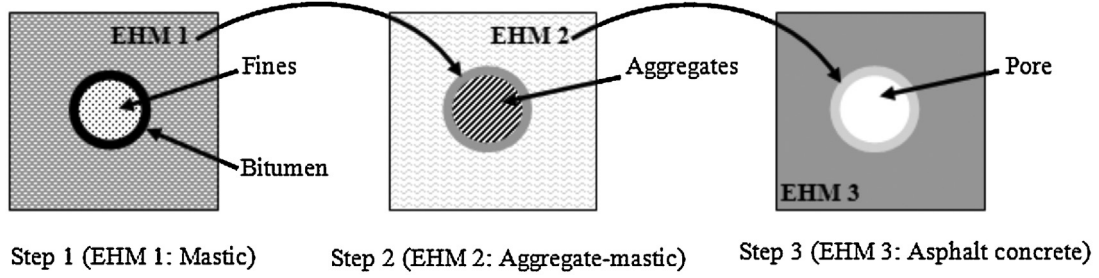
Fig. 4 – Schematic representation of the step-by-step homogenization process.

$$\begin{cases} \left\langle \varepsilon_i^{sph} \right\rangle = \dfrac{F_i}{F_{n+1}} \mathbb{1} \mathbf{E_0} = \mathbb{A}_i^{sph} \mathbf{E_0} \\ \left\langle \varepsilon_i^{dev} \right\rangle = \dfrac{1}{A_{n+1}} \left(A_i - \dfrac{21}{5} \dfrac{R_i^5 - R_{i-1}^5}{(1 - 2v_i)(R_i^3 - R_{i-1}^3)} B_i \right) \mathbb{1} \mathbf{E_0} = \mathbb{A}_i^{dev} \mathbf{E_0} \end{cases}$$

(5)

where R_i denotes the radius of the phase i, the coefficients A_i, B_i and F_i are constants defined in Appendix A and $\mathbb{1}$ is the identity tensor of 4th order.

Once the strain localization tensors of the secondary problems are known, the localization tensor of the global problem can be derived from Eq. (3). Then, the use of Eq. (1) combined to Eq. (4) allows the computation of the effective bulk and shear moduli of the heterogeneous material. Eq. (6) presents the summarized form expressions of the effective mechanical properties.

$$\begin{cases} k^{hom} = \left(f_a k_a \mathbb{A}_a^{sph} + f_m k_m \mathbb{A}_m^{sph} f_p k_p \mathbb{A}_p^{sph} \right) : \\ \qquad \times \left(f_a \mathbb{A}_a^{sph} + f_m \mathbb{A}_m^{sph} f_p \mathbb{A}_p^{sph} \right)^{-1} \\ \mu^{hom} = \left(f_a \mu_a \mathbb{A}_a^{dev} + f_m \mu_m \mathbb{A}_m^{dev} f_p \mu_p \mathbb{A}_p^{dev} \right) : \\ \qquad \times \left(f_a \mathbb{A}_a^{dev} + f_m \mathbb{A}_m^{dev} f_p \mathbb{A}_p^{dev} \right)^{-1} \end{cases}$$

(6)

where $\mathbb{A}^{sph}$ and $\mathbb{A}^{dev}$ are the strain localization tensors of respectively the hydrostatic pressure and simple shear problems.

2.2. Successive homogenization approach

In this section, we present a different approach for the prediction of the effective mechanical properties of the elastic composite based upon a successive homogenization method. The latter consists on a step-by-step homogenization process which involves different REVs and homogenization schemes for each step. The output effective solution computed in step (i) is considered as an input data for the following step (i + 1). The advantage of such an approach is essentially to trim down the complex problem and to track its complexities in different stages allowing therefore an "easy" and classic homogenization of the global problem. Note that this model was previously used by Alam and Hammoum [17] for the prediction of the viscoelastic properties of Hot Mix Asphalt which is assumed as a composite of four phases (fines, bitumen, aggregates and voids). Fig. 4 illustrates the different steps of the successive homogenization process considered herein. The steps correspond to RVEs, each of which, composed of three phases, is a composite inclusion embedded in a matrix.

In the first step, bitumen and fines are homogenized together to obtain the mastic (EHM 1). Then, the latter is considered as a layer for the aggregates in the second step. Accordingly, the new homogenized medium is a mixture of aggregates and mastic (EHM 2). Finally, the porosity is taken into account in the third step as an inclusion (void) surrounded by the EHM 2 derived from the second homogenization step.

Since the inclusion is composite, we used a generalized self-consistent scheme for each step of the homogenization process; the effective bulk and shear moduli of the composite can be predicted using a $(n + 1)$-phase model (with $n = 2$) according to the following:

$$\begin{cases} k^{hom} = k_n + \dfrac{(R_{n-1}^3/R_n^3)(k_{n-1} - k_n)}{1 + ((R_n^3 - R_{n-1}^3)/R_n^3)((k_{n-1} - k_n)/(k_n + 4/3\mu_n))} \\ A \left(\dfrac{\mu^{hom}}{\mu_n} \right)^2 + B \left(\dfrac{\mu^{hom}}{\mu_n} \right) + C = 0 \end{cases}$$

(7)

where the expressions of the coefficients A, B and C are given in Appendix A. Note that in this particular case of $n = 2$, the equations yield to the classical solution of the 3-phase model [12].

2.3. Extension to the viscoelasticity

The well-known correspondence principle is widely used for viscoelastic composites in order to transpose the effective elastic solutions from the elasticity to the viscoelasticity [21–23]. The correspondence is essentially based on the similitude noticed between the elastic constitutive law, on the one hand, and that of the viscoelasticity expressed in Laplace–Carson domain. It was highlighted, however, by many researches that the determination of the viscoelastic effective creep and relaxation moduli is not often straightforward since it often required rational fraction forms of the elastic effective solutions of the Laplace Carson transform in order to make possible the computation of the inverse transform. The works of Hashin [24] established a simple correspondence principle relating the effective complex moduli to effective elastic one of composites. Accordingly, in order to obtain the effective complex moduli of a viscoelastic heterogeneous material, the elastic i-phase moduli k_i and μ_i have to be replaced by the complex i-phase moduli $k_i^*(i\omega)$ and $\mu_i^*(i\omega)$. Accordingly, the constitutive law of the viscoelastic composite can be written as follows:

$$\tilde{\sigma}_{ij} = \tilde{\lambda}^*(i\omega)\tilde{\varepsilon}_{kk}\delta_{ij} + 2\tilde{\mu}^*(i\omega)\tilde{\varepsilon}_{ij}$$

(8)

Table 1 – Summary of the mechanical properties of asphalt constituents.				
Materials	Stiffness modulus (GPa)	Poisson's ratio	Shear modulus (GPa)	Compressibility modulus (GPa)
Aggregates	105.500	0.25	42.233	70.053
Fines	55.200	0.15	2.400	26.285
Bitumen	–	0.33	–	–

where i is the complex variable ($i^2 = 1$); $\tilde{\lambda}^*$ and $\tilde{\mu}^*$ are respectively the Lamé coefficient and the complex shear modulus of the viscoelastic composite ω is the solicitation frequency.

3. Illustration on a high rate recycled HMA

3.1. Materials description

The GSCS-based approach is illustrated on a laboratory case of a hot recycled asphaltic concrete (BBSG 0/10) previously considered by the authors [4]. The recycled mixture includes 70% of RAP and 30% of virgin materials (bitumen + aggregates). The richness modulus of the recycled HMA is equal to 3.6 with a total bitumen content of 5.74% ppc (by weight of dry aggregates). The recycled HMA is a 20/30 penetration grade bitumen whereas the virgin and the RAP bitumens are 160/220 and 10/20 penetration grades respectively. It shall be emphasized that the manufacture parameters, namely the mixing temperature and the mixing time, were calibrated such as two experimental configurations (good blending and bad blending) and they can be studied. Table 1 summarizes the input data of the asphalt constituents.

3.2. Rheological measurements

Rheological tests were performed on three kinds of bitumen: the virgin bitumen, the RAP bitumen and the homogeneous blend derived from the recycled asphaltic concrete. The RAP and homogeneous bituminous binders were obtained by a conventional extraction method using an asphalt analysator and then recovered by vacuum distillation using a rotary evaporator according to the standard specifications, respectively NF EN 12697-1 and NF EN 12697-3. Afterwards, the rheological experiments were carried out using a Bohlin Dynamic Shear Rheometer (DSR) from Malvern in mode plate and plate geometry (8 mm, gap = 1 mm) within the linear viscoelastic (LVE) domain in the frequency range 0.1–10 Hz and for temperatures varying between 5 and 60 °C.

4. Results and discussion

4.1. Case of a homogeneous blend

The sieves curves of virgin, RAP and recycled aggregates are presented in Fig. 5.

4.1.1. Rheological results (complex modulus)
The isotherms and isochrones of shear complex modulus μ^* of the three bituminous binders are depicted in Fig. 6. It can be seen from these plots that the complex modulus of the three binders exhibits the same trends with regard to the

temperature on the one hand and the frequency solicitation on the other one. The higher the temperature, the lower is the rigidity of the bitumen. On the other side, the higher the frequency, the higher is the complex modulus. Moreover, one can notice that the RAP bitumen presents the higher rigidity whereas the recycled bitumen lies between the virgin and the RAP curves. This is due to the aging phenomenon experienced
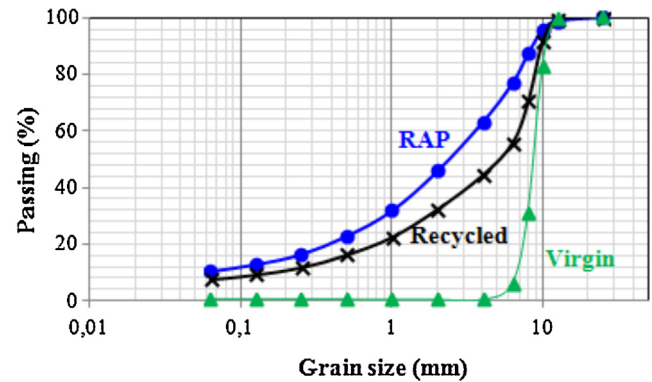

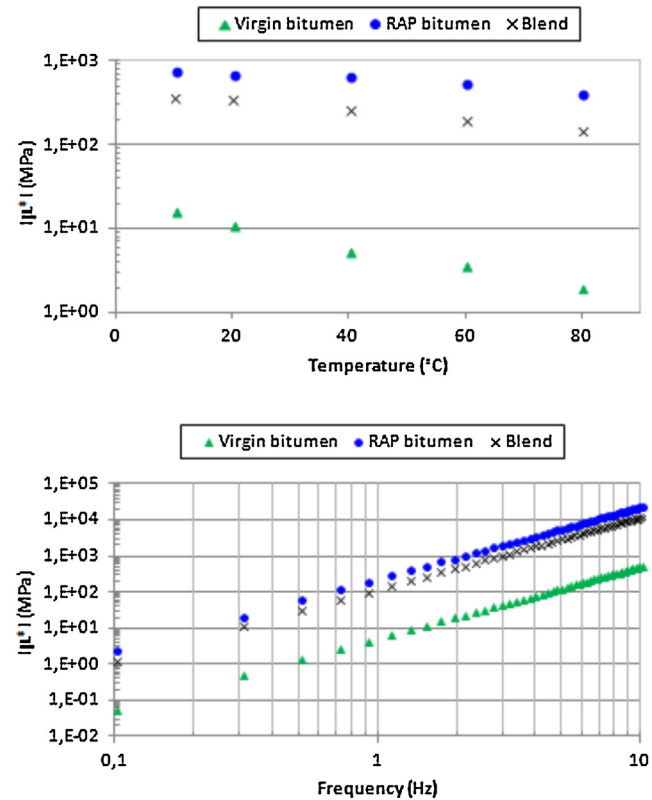Fig. 5 – Sieve curves of virgin, RAP and blended aggregates.

Fig. 6 – Results of the shear complex modulus measurements: isotherms at f = 1.59 Hz (upper curves), and isochrones at T = 10 °C (lower curves).
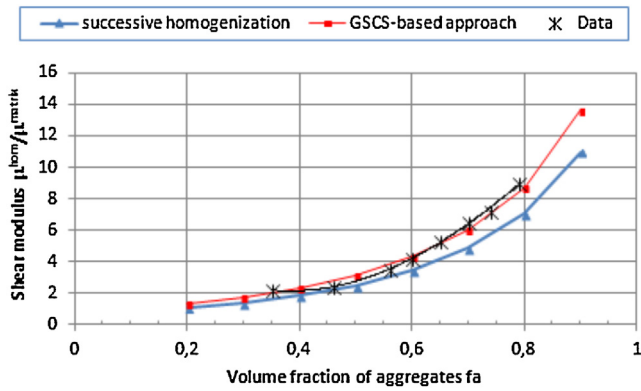
Fig. 7 – Effective elastic shear modulus predicted by the GSCS-based approach and the successive homogenization, and its comparison with the experimental data.

Table 2 – Literature data used for the comparison with the homogenization approaches.

	Matrix (epoxy resin)	Inclusion (normalized Sand)
Stiffness modulus (GPa)	2.518	73.08
Poisson's ratio	0.413	0.172
Source [25].		

by the RAP bitumen during its life service through the daily repetitive mechanical and thermal loads which have affected the hardness of the bitumen.

4.1.2. Comparison with the successive homogenization (elasticity case)

Fig. 7 depicts the results of the effective elastic shear modulus μ^{hom} with a monolayer rigid inclusion in comparison with the predictions given by the successive homogenization approach. It can be outlined that the two models correlate very well for an aggregate volume fraction less than 35%. However, when the inclusion concentration is more important, a higher deviation can be noticed between the two approaches. This finding could be explained by the interaction effect between the different phases which is more highlighted when the aggregates volume fraction becomes important. In fact, when the volume fraction is less than 35%, the aggregates are somewhat diluted in the porous matrix, so the interaction effect is not sufficiently strong and the different phases of the composite could therefore be assumed as independent "packages" which could be homogenized separately through a step-by-step method as preceded by the aforementioned successive
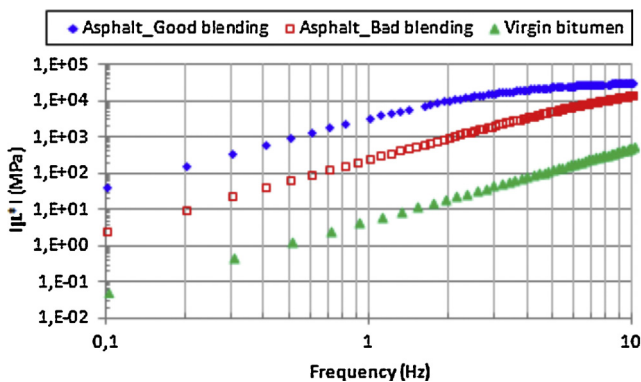
homogenization approach. However, when the volume fraction becomes more important, some bonds and interactions may be built between the different phases and it requires, as a consequence, to be taken into account in the homogenization process of the composite.

In order to arbitrate more objectively between the two approaches, some experimental results of effective shear moduli corresponding to a homogenized granular medium with two phases were gathered from the literature (Table 2) and used herein for the confrontation of the homogenization methods with the experience in the particular elastic case [25].

The data of the effective elastic shear modulus are presented in Fig. 7 by asterisk black marks. It can be noticed that the tendency curve fitting the experimental results is closer to the GSCS-based approach than the successive homogenization model especially for high aggregates fraction volume ($fa > 55\%$). Although the successive homogenization method has the advantages of being much simpler and less cumbersome than the GSCS-based model, it can unfortunately provide inaccurate predictions of the apparent mechanical properties and performances of the heterogeneous material and yields therefore to unsafe road pavement design. Note that the successive homogenization method underestimates the rigidity of the composite of about 20% when the aggregates volume fraction is equal to 80%. On the basis of this simple case study of elastic heterogeneous medium, the GSC-based approach is proved to be the best appropriate method for the prediction of effective mechanical properties of the heterogeneous material. In the next section, this approach is adopted for the estimation of the equivalent shear modulus of the recycled asphaltic concrete.

4.2. Effect of the level of blending (case of BBSG asphalt concrete)

Plots of Fig. 8 present the evolution versus the frequency of the equivalent shear modulus of the recycled asphaltic concrete base upon the GSCS-based approach. The calculations were performed by considering two configurations, namely the monolayer rigid inclusion (case of "good" blending) and the bilayer rigid inclusion (case of "bad" blending). It can be noticed from this figure that the case of a homogeneous blend exhibits higher complex shear modulus of the recycled asphalt in comparison with the "bad" recycled asphalt. This finding let deduce that the rigidity of the composite is significantly improved when the virgin and RAP binders are well blended together during the manufacture process yielding thereby a unique continuous layer around the aggregates. Nevertheless, when the binders are not well blended, the recycled bitumen is split into two different layers with different properties and behaves therefore somewhat like two "unknown" and

Fig. 8 – Effective complex shear modulus evolution as a function of frequency for T = 10 °C, results for recycled asphalt (case of good and bad blending), and virgin bitumen.

discontinuous materials. This could affect the shear modulus of the overall composite.

5. Conclusions

In this paper, a GSCS-based micromechanical model was presented for the investigation of the mechanical behavior of a high rate recycled HMA mixture. Motivated by the knowledge of the rheological properties of three different binders, this study aims to predict by the means of a multiscale modeling the equivalent mechanical properties of a recycled porous composite taking into account the microstructure configurations resulting from the blending level of the virgin bitumen into the RAP binder during the manufacture process. Some conclusions can be drawn at the end of this research:

- The GSCS-based model, based on a one-step homogenization, is shown to be suitable and efficient to predict the effective shear modulus of the heterogeneous material. In particular, the comparison of the developed approach in the elastic case has shown a good agreement with the homogenization data gathered from literature.
- Although it has numerical complexity, the GSCS-based model was proved to be safer than the multi-steps homogenization since it allows taking into account the possible interactions which could occur between the different phases of the composite especially when the inclusion volume fraction is not negligible.
- The blending level between the new and the old bituminous binders can have significant effects on the estimation of the effective shear modulus of the recycled final product. The illustration on the high rate recycled HMA case has shown considerable differences noticed in the evaluation of the equivalent shear modulus between "good" and "bad" recycled asphaltic concretes. This finding highlights the strong relationship between the asphalt manufacture process on the one hand and the viscoelastic performances of the recycled asphalt on the other one.

However, several limitations of this research are needed to be mentioned such as the lack of experimental data of shear complex modulus of recycled asphalt to compare with the GSCS-based approach results. Furthermore, the size distribution and the random morphological characteristics of aggregates were not taken into account in the present study. Accordingly, it is worthwhile to carry on complementary experimental researches for the measurement of the mechanical properties of the recycled asphalt, and to further investigate the aggregates properties and take them in consideration in the micromechanical model.

Appendix A. Case of n-layered composite sphere (average strains constants and effective shear modulus solutions) [14]

A.1. Coefficients A_i, B_i, F_i

See Fig. A.1.

$$F_i = \frac{1}{Q_{11}^n} F_{n+1} \tag{A.1}$$

$$Q^{(k)} = \prod_{j=1}^{(k)} N^{(j)} \tag{A.2}$$

$$N^{(k)} = \frac{1}{3K_{k+1} + 4\mu_{k+1}} \begin{pmatrix} 3K_k + 4\mu_{k+1} & \frac{4}{R_k^3}(\mu_{k+1} - \mu_k) \\ 3(K_{k+1} - K_k)R_k^3 & 3K_{k+1} + 4\mu_k \end{pmatrix} \tag{A.3}$$

$$A_i = P_{22}^{(n)} \frac{A_{n+1}}{P_{11}^{(n)} P_{22}^{(n)} - P_{12}^{(n)} P_{21}^{(n)}} P^{(i-1)}; \quad i = [1, n+1] \tag{A.4}$$

$$B_i = -P_{21}^{(n)} \frac{A_{n+1}}{P_{11}^{(n)} P_{22}^{(n)} - P_{12}^{(n)} P_{21}^{(n)}} P^{(i-1)}; \quad i = [1, n+1] \tag{A.5}$$

$$P^n = \prod_{i=1}^n M^i$$

and

$$M^{(k)} = \frac{1}{5(1 - v_{k+1})}$$

$$\times \begin{pmatrix} \frac{C_k}{3} & \frac{R_k^2(3b_k - 7C_k)}{5(1 - 2v_k)} & -\frac{12\alpha_k}{R_k^5} & \frac{4(f_k - 27\alpha_k)}{15(1 - 2v_k)R_k^3} \\ 0 & \frac{(1 - 2v_{k+1})b_k}{7((1 - 2v_k)} & -\frac{20((1 - 2v_{k+1})\alpha_k}{7R_k^7} & -\frac{12\alpha_k(1 - 2v_{k+1})}{7(1 - 2v_k)R_k^5} \\ \frac{R_k^5\alpha_k}{2} & \frac{R_k^7(2a_{k+} - 147\alpha_k)}{70(1 - 2v_k)} & \frac{d_k}{7} & \frac{R_k^2[105(1 - v_{k+1}) + 12\alpha_k(7 - 10v_{k+1}) - 7e_k]}{35(1 - 2v_k)} \\ -\frac{5}{6}(1 - 2v_{k+1})\alpha_k R_k^3 & 7(1 - 2v_k)\alpha_k R_k^5 & 0 & \frac{e_k(1 - 2v_{k+1})}{3(1 - 2v_k)} \end{pmatrix} \tag{A.6}$$
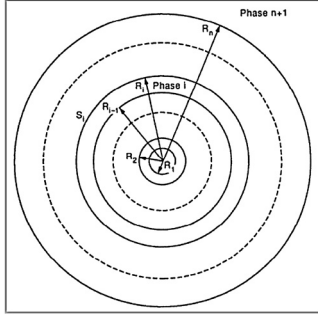
Fig. A.1 – The *n*-layered spherical inclusion embedded in an infinite matrix
Source [14].

---

with

$$a_k = (7 + 5v_k)(7 - 10v_{k+1})\frac{\mu_k}{\mu_{k+1}} - (7 - 10v_k)(7 + 5v_{k+1})$$

$$b_k = 4(7 - 10v_k) + (7 + 5v_k)\frac{\mu_k}{\mu_{k+1}}$$

$$c_k = (7 - 5v_{k+1}) + 2(4 + 5v_{k+1})\frac{\mu_k}{\mu_{k+1}}$$

$$d_k = (7 - 5v_{k+1}) + 4(7 + 10v_{k+1})\frac{\mu_k}{\mu_{k+1}} \qquad \text{(A.7)}$$

$$e_k = 2(4 - 5v_k) + (7 + 5v_k)\frac{\mu_k}{\mu_{k+1}}$$

$$f_k = (4 - 5v_k) + (7 - 5v_{k+1}) - (4 - 5v_{k+1})(7 - 5v_k)\frac{\mu_k}{\mu_{k+1}}$$

$$\alpha_k = \frac{\mu_k}{\mu_{k+1}} - 1$$

A.2. Effective shear modulus solution according to the (n + 1)-phase model

$$A\left(\frac{\mu^{hom}}{\mu_n}\right)^2 + B\left(\frac{\mu^{hom}}{\mu_n}\right) + C = 0 \qquad \text{(A.8)}$$

with

$$
\begin{aligned}
A =&\ 4R_n^{10}(1 - 2v_n)(7 - 10v_n)Z_{12} + 20R_n^7(7 - 12v_n + 8v_n^2)Z_{42} \\
&+ 12R_n^5(1 - 2v_n)(Z_{14} - 7Z_{23}) + 20R_n^3(1 - 2v_n)^2Z_{13} \\
&+ 16(4 - 5v_n)(1 - 2v_n)Z_{43} \\
B =&\ 3R_n^{10}(1 - 2v_n)(15v_n - 7)Z_{12} + 60R_n^7(v_n - 3)v_nZ_{42} \\
&- 24R_n^5(1 - 2v_n)(Z_{14} - 7Z_{23}) - 40R_n^3(1 - 2v_n)^2Z_{13} \\
&- 8(4 - 5v_n)(1 - 2v_n)Z_{43} \\
C =&\ -R_n^{10}(1 - 2v_n)(5v_n + 7)Z_{12} + 10R_n^7(7 - v_n^2)Z_{42} \\
&+ 12R_n^5(1 - 2v_n)(Z_{14} - 7Z_{23}) + 20R_n^3(1 - 2v_n)^2Z_{13} \\
&- 8(7 - 5v_n)(1 - 2v_n)Z_{43}
\end{aligned} \qquad \text{(A.9)}
$$

where

$$Z_{\alpha\beta} = P_{\alpha1}^{(n-1)}P_{\beta2}^{(n-1)} - P_{\beta1}^{(n-1)}P_{\alpha2}^{(n-1)}; \quad \alpha, \beta \in [1, 4] \qquad \text{(A.10)}$$

REFERENCES

[1] J.W. Button, D.N. Little, C.K. Estakhri, Hot In-Place Recycling of Asphalt Concrete National Cooperative Research Program Synthesis of Highway Practice 193, Transportation Research Board, Washington, DC, 1994.

[2] A. Vanelstraete, J. De Visscher, M. Fernandez, J.A. Soto, L. De Bock, Selection of binders for asphalt mixes with reclaimed asphalt as studied in the paramix project, in: 3rd Eurasphalt & Eurobitume congress, Vienna-Paper 154, 2004.

[3] D.N. Little, R.J. Holmgreen, J.A. Epps, Effect of recycling agents on the structural performance of recycled asphalt concrete materials, Proceedings of the Association of Asphalt Paving Technologists 50 (1981) 32–63.

[4] A. Eddhahak-Ouni, A. Dony, J. Colin, et al., Assessment of experimental approach for qualitative characterization of a high rate recycled asphalt mixture, Road Material and Pavement Design 13 (3) (2012) 566–575.

[5] A. Eddhahak-Ouni, A. Dony, J. Colin, et al., On a laboratory experimental protocol for qualitative characterization of high rate recycled asphalt mixtures, in: 5th Eurasphalt & Eurobitume Congress, Istanbul, 13–15 June, 2012.

[6] C. Huet, Coupled size and boundary-condition effects in viscoelastic heterogeneous and composite bodies, Mechanics of Materials 31 (1999) 787–829.

[7] Shell Bitumes, Techniques et Utilisations, 1991.

[8] L. Franken, A. Vanelstraete, Relation between mix stiffness and binder complex modulus, the rheology of bituminous binders, in: European Workshop, Brussels, 5–7 April, 1995.

[9] H. Di Benedetto, P. Des Croix, Binder-mix rheology: limits of linear domain, nonlinear behavior, in: Eurasphalt and Eurobitume Congress, 1996.

[10] Q. Xu, Solaimanian, Modeling linear viscoelastic properties of asphalt concrete by the Huet–Sayegh model, International Journal of Pavement Engineering 10 (2009) 401–422.

[11] H. Di Benedetto, F. Olard, C. Sauzéat, B. Delaporte, Linear viscoelastic behavior of bituminous materials: from binders to mixes, Road Materials and Pavement Design 163 (2004) 163–202.

[12] W.G. Buttlar, D. Bozkurt, G.G. Al-Khateeb, A.S. Waldhoff, Understanding asphalt mastic behavior through micromechanics, Transportation Research Record 1681 (1999) 157–166.

[13] R.M. Christensen, K.H. Lo, Solutions for effective shear properties in three phase sphere and cylinder models, Journal of the Mechanics and Physics of Solids 27 (1979) 315–330.

[14] E. Hervé, A. Zaoui, *n*-Layered inclusion based micromechanical modeling, International Journal of Engineering Science 31 (1993) 1–10.

[15] N. Shashidar, A. Shenoy, On using micromechanical models to describe dynamic behavior of asphalt mastics, Mechanics of Materials 34 (2002) 657–669.

[16] A. Lachihab, A Numerical Model for the Two-Phase Composites Matrix-Rigid Inclusions: Application to the Determination of the Elastic and Fatigue Properties of the Bituminous Materials, (Ph.D. thesis), Ecole Nationale des Ponts et Chaussées, France, 2004.

[17] S.Y. Alam, F. Hammoum, Viscoelastic properties of asphalt concrete using micromechanical self-consistent model, Archives of Civil and Mechanical Engineering 15 (2015) 272–285.

[18] Ch. Pichler, R. Lackner, E. Aigner, Generalized self-consistent scheme for upscaling of viscoelastic properties of highly-filled matrix-inclusion composites – application in the context of multiscale modeling of bituminous mixtures, Composites Part B 43 (2012) 457–464.

[19] J. Navaro, Cinétique de mélange des enrobés recyclés et influence sur les performances mécaniques, (Ph.D. thesis), ENSAM, France, 2011.

[20] R.M. Christensen, K.H. Lo, Journal of Mechanics and Physics of Solids 27 (1979) 315, Erratum.

[21] J. Mandel, Cours de mécanique des milieux continus, Gauthier-Villars, 1966.

[22] E. Lee, Stress analysis for linear viscoelastic materials, Rheologica Acta 1 (4) (1961) 426–430.

[23] S. Beurthey, A. Zaoui, Structural morphology and relaxation spectra of viscoelastic heterogeneous materials, European Journal of Mechanics – A/Solids 19 (1) (2000) 1–16.

[24] Z. Hashin, Complex moduli of viscoelastic composites – I. General theory and application to particulate composites, International Journal of Solids and Structures 6 (1970) 539–552.

[25] H.G. Nguyen, Approche micromécanique pour la modélisation du comportement élastoplastique des composites: Application aux mortiers de résine, (Ph.D. thesis), Cergy-Pontoise, France, 2008.